

# Development of $\text{In}_2\text{O}_3$ -based Catalysts for $\text{CO}_2$ -based Methanol Production

Matthias S. Frei<sup>§</sup>, Cecilia Mondelli, and Javier Pérez-Ramírez\*

<sup>§</sup>SCS-DSM Award for best poster presentation in Catalysis Science & Engineering

**Abstract:**  $\text{CO}_2$  valorization into chemicals and fuels is a key area in current academic and industrial research, with thermocatalytic hydrogenation to methanol comprising one of the most advanced routes. Life-cycle analysis coupled to the framework of planetary boundaries has recently confirmed the sustainability of this process in absolute terms, emphasizing the need for cheaper  $\text{CO}_2$  and renewable  $\text{H}_2$  and for a catalytic system embracing high activity, selectivity, and durability to meet economic requirements. Herein, our research efforts aimed to gather atomic-level understanding of electronic and geometric properties of active sites in breakthrough  $\text{In}_2\text{O}_3$ -based catalytic systems guiding their development are reviewed. In-depth mechanistic elucidations identified limited hydrogen activation ability as well as water-driven sintering as limitations of pure  $\text{In}_2\text{O}_3$ . The former aspect was successfully addressed by adding through coprecipitation a minimal amount of palladium, forming tiny clusters strongly anchored to the oxide lattice leading to an unprecedented sustained methanol productivity. The use of monoclinic zirconia as a carrier, enabling high  $\text{In}_2\text{O}_3$  dispersion in two-dimensional nanostructures, inducing the formation of additional active sites on  $\text{In}_2\text{O}_3$ , and contributing to  $\text{CO}_2$  activation, offered an efficient way to further boost activity and tackle  $\text{In}_2\text{O}_3$  sintering. Overall, our findings set solid grounds to rationally design a supported and promoted  $\text{In}_2\text{O}_3$  catalyst holding bright prospects for use at a large scale.

**Keywords:**  $\text{CO}_2$  hydrogenation · Green methanol · Heterogeneous catalysis · Indium oxide · Promotion



**Matthias Frei** is a PhD student in the group of Prof. Pérez-Ramírez. His research focuses on the development of heterogeneous catalysts for the sustainable production of methanol from carbon dioxide.



**Dr. Cecilia Mondelli** is a lecturer in the group of Advanced Catalysis Engineering at ETH Zurich. Her research is centered on the valorization of renewable feedstocks, such as  $\text{CO}_2$  or biomass into chemicals and fuels.



**Prof. Javier Pérez-Ramírez** holds the Chair of Catalysis Engineering at ETH Zurich. His research pursues the design of heterogeneous catalysts and reactor concepts devoted to sustainable technologies.

## $\text{CO}_2$ -based Methanol Production: A Sustainable Path Forward

Aiming to mitigate global warming and fulfil the growing demand for products and energy more sustainably, academia, the chemical industry, and the energy sector are directing substantial research efforts to develop technologies able to utilize  $\text{CO}_2$  as a feedstock.<sup>[1]</sup> In this context, methanol is receiving widespread attention owing to its essential role as a platform chemical and its potential as a fuel.<sup>[2]</sup> Its production through the thermocatalytic hydrogenation of  $\text{CO}_2$  with renewable  $\text{H}_2$  has been regarded as highly relevant since the start, due to the readily available infrastructure in the chemical industry. To determine its potential to replace fossil-fuel based technologies in the coming decades,<sup>[3]</sup> we have conducted, in collaboration with a system engineering group at the ETH Zurich, accurate process modelling and assessment through economic and environmental metrics to identify technical barriers and define performance targets, which provide valuable guidelines for the development of suitable catalytic materials. Our analysis for the first time considered this chemical technology on a global scale *via* state-of-the-art life-cycle assessment (LCA) as well as the application of planetary boundaries (PB) to determine absolute sustainability.<sup>[4]</sup> In this study, the  $\text{Cu-ZnO-Al}_2\text{O}_3$  catalyst, industrially applied in methanol synthesis from syngas, was selected due to the availability of copious kinetic data for this system in  $\text{CO}_2$  hydrogenation too.

Based on conventional LCA (Fig. 1a),  $\text{CO}_2$ -based methanol appears more expensive than fossil-based methanol. Hydrogen and, to a lesser extent,  $\text{CO}_2$  emerge as the main contributors to the total methanol production cost, with renewable hydrogen obtained from water electrolysis powered by wind energy and  $\text{CO}_2$  captured from a coal power plant being the most economic feedstock options (Fig. 1a).

\*Correspondence: Prof. Dr. J. Pérez-Ramírez, E-mail: jpr@chem.ethz.ch

Institute for Chemical and Bioengineering, Department of Chemistry and Applied Biosciences, ETH Zurich, Vladimir-Prelog-Weg 1, CH-8093 Zurich, Switzerland

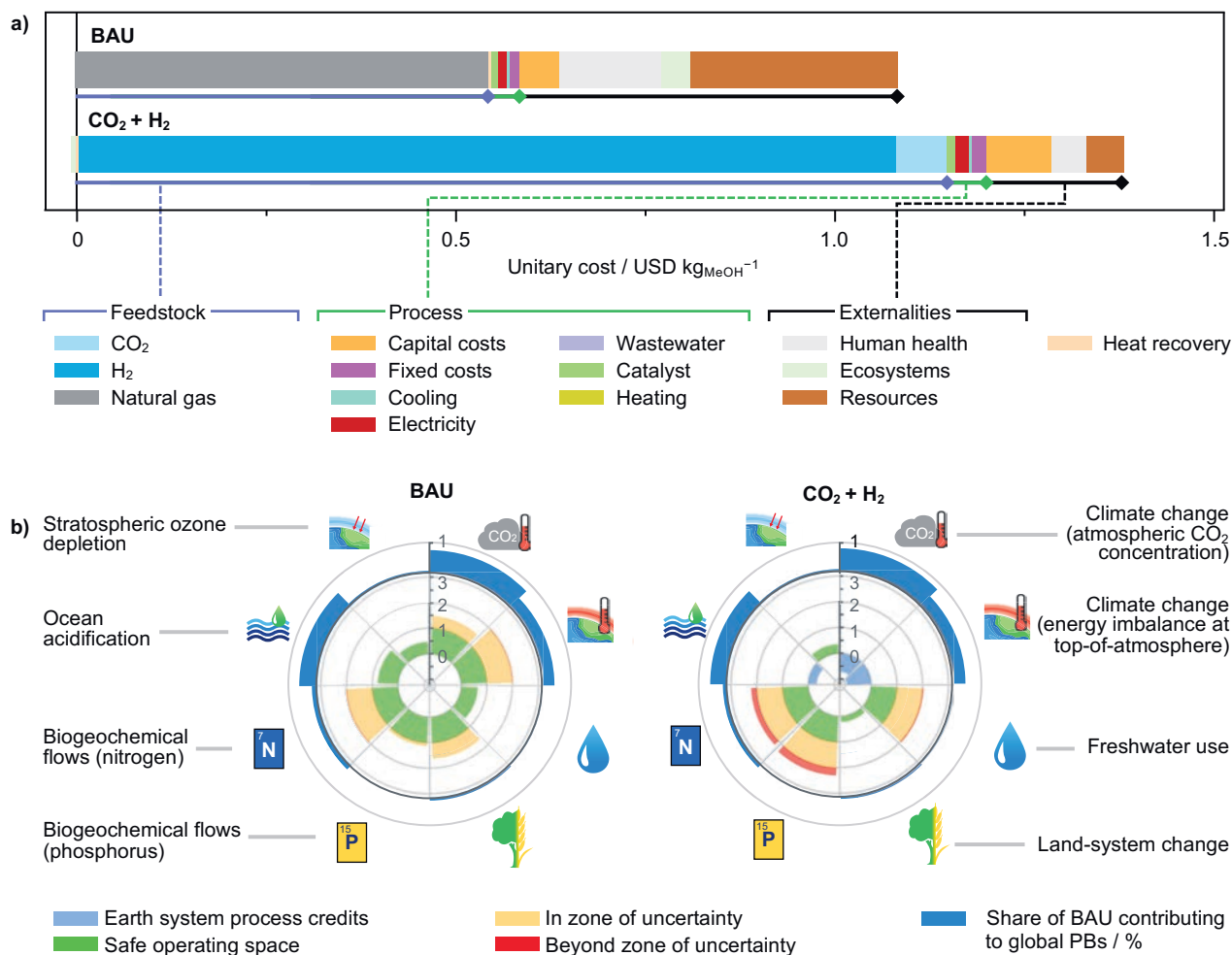


Fig. 1. a) Total cost, including externalities, of fossil-based methanol from syngas (business as usual, BAU) and CO<sub>2</sub>-based methanol produced using renewable hydrogen obtained using wind power, together with the cost and externalities breakdowns. b) Current impact of fossil-based methanol production on the planetary boundaries, along with the performance of the green methanol process. The normalization applied scales the level of transgression to the maximum level of transgression across technologies and Earth systems. Negative contributions, *i.e.* environmental credits, towards climate change and ocean acidification are associated with technologies that are carbon-negative on a cradle-to-gate basis due to the use of captured CO<sub>2</sub>. The outer rings of the radar plots represent the share of the safe operating space allocated to methanol production in the different Earth systems on a percent scale.

Hence, bringing this emerging technology towards industrialization will rely on cheap hydrogen production as well as on catalysts that utilize hydrogen in an efficient manner. The development of a more efficient CO<sub>2</sub> capture technology, or the deployment of the methanol synthesis process vicinal to steel or lime production sites, which generate flue gases with extraordinarily high concentration of CO<sub>2</sub>, will also be instrumental to this end. After this traditional techno-economic analysis, we ventured to explore whether such a technology would be sustainable in global terms. Thus, we incorporated the LCA data within the recently introduced framework of planetary boundaries, investigating how a green methanol synthesis process would accommodate within the natural constraints imposed by the Earth's ecosystems (Fig. 1b). In this context, it is evident that a CO<sub>2</sub>-based process bears much brighter environmental prospects than the commercial route. Not only are more (5 vs. 3 out of 8) planetary boundaries met, but also environmental credits are generated in ocean acidification and the currently most heavily transgressed climate change-related systems, thanks to the utilization of CO<sub>2</sub> as a feedstock. Some collateral damage arises through the transgression of the boundaries of phosphorous and nitrogen flows and freshwater consumption, but this burden shift appears of minor concern, because methanol synthesis contributes to these boundaries only to a marginal extent (see outer rings in the radar plots). Determining that this process would bring ecological, and, with more stringent legislation for CO<sub>2</sub> emissions, potentially economic benefits, places

urgency not only in ensuring cheaper feedstocks acquisition but also in the identification of disruptive catalytic technologies. Indeed, the commercial methanol synthesis catalyst used for the purpose of modelling is intrinsically unsuited for a CO<sub>2</sub>-based process due to severe selectivity and stability limitations.

Aiming to curtail these issues, our research focused on In<sub>2</sub>O<sub>3</sub>. Following early theoretical investigations and preliminary experimental insights,<sup>[5,6]</sup> our group initially explored the potential of this active phase in a comprehensive manner.<sup>[7]</sup> Within that study, extraordinarily high selectivity and stability were evidenced for In<sub>2</sub>O<sub>3</sub> when supported on monoclinic ZrO<sub>2</sub>, and the active catalyst site was ascribed to oxygen vacancies formed on the surface of the active reducible oxide. Nevertheless, clear structure–performance relationships remained elusive at that point. Hereon, we will overview how we more recently unraveled the mechanistic origin of the high methanol selectivity on In<sub>2</sub>O<sub>3</sub>,<sup>[8]</sup> how the insights gained permitted us to atomically engineer a robust palladium-promoted system,<sup>[9]</sup> and how we rationalized the uniqueness of monoclinic zirconia as the carrier,<sup>[10]</sup> setting solid grounds for the rational design of a practical catalyst meeting the demands of a large-scale CO<sub>2</sub>-based methanol synthesis process.

### Kinetics of CO<sub>2</sub> Hydrogenation over Bulk In<sub>2</sub>O<sub>3</sub>

A sound mechanistic understanding is paramount for the design of catalysts for CO<sub>2</sub>-based methanol synthesis, since this re-

action has to be carried out in a kinetically-controlled regime. Indeed, the thermodynamic equilibrium highly favors the undesired reverse water-gas shift (RWGS) reaction over the hydrogenation to methanol under the conditions commonly applied *ca.* 573 K, 5 MPa, molar  $H_2:CO_2 = 3-4$ . Consequently, in order to pinpoint crucial performance descriptors and identify parameters for catalyst optimization, our initial research efforts centered on unraveling the mechanism and reaction kinetics of methanol synthesis over pure  $In_2O_3$ .<sup>[8]</sup> Density functional theory (DFT) analysis uncovered that vastly diverse energies are required to remove the 12 oxygen atoms present at the outmost layer of a unit cell of the most stable  $In_2O_3(111)$  termination (Fig. 2a). The creation of an oxygen vacancy in the most favorable position generates the active site of this catalyst, specifically an  $In_3O_5$  ensemble. Storage of electrons is possible within the indium trimer and, thus, heterolytically-split hydrogen can be stabilized (Fig. 2b).<sup>[11]</sup> This opens up a reaction mechanism for the hydrogenation of  $CO_2$  to methanol through three consecutive hydride-proton transfers (Fig. 2c), which comprise the rate-determining steps of the whole transformation. Although the catalyst can also mediate the reverse water-gas shift reaction, the activation energy predicted for the latter is higher than for methanol synthesis, in good agreement with experimentally attained values (Table 1). Further experimental kinetic analyses revealed a pronounced performance dependency on the hydrogen concentration in the feed, owned to the high energy barriers for its activation, and a significant inhibiting effect of water, in line with its hindered desorption. The ease of  $CO_2$  adsorption and methanol desorption was reflected in their negligible inhibiting role on methanol synthesis. Within these studies, CO and  $H_2O$  were uncovered as agents responsible for catalyst deactivation, the former causing over-reduction of the oxide surface if present in sufficiently high concentrations (>10 vol.%), the latter provoking sintering of  $In_2O_3$  through condensation of surface hydroxyl groups. These findings hold practical relevance, because both molecules are likely to be present to appreciable extents in the reactor due to outlet stream recycling. Therefore, rendering hydrogen activation easier and improving the resilience of the catalyst to carbon monoxide and water emerged as priority aspects for catalyst optimization.

### Promotion of $In_2O_3$ by Palladium

To foster hydrogen activation over  $In_2O_3$ -based catalysts, various (noble) metal promoters were tested, among which palladium was identified as the best candidate.<sup>[9]</sup> With only 0.75 wt.% of this metal introduced by coprecipitation (CP) or dry impregnation (DI), a three-fold increase in the methanol productivity was attained compared to bulk  $In_2O_3$ . However, only the CP material maintained the activity enhancement solely directed to methanol synthesis upon extended operation, whereas the DI solid displayed a rapid loss in methanol productivity due to a progressively higher CO selectivity (Fig. 3a). Based on structural, spectroscopic

and microscopy analysis, palladium was found to be atomically dispersed in the fresh CP material, with a fraction of the promoter being incorporated within the  $In_2O_3$  lattice and another fraction being deposited onto its surface, and to form clusters of only 2–4 atoms in size upon use in the reaction. In case of the DI catalyst, more severe sintering of the promoter into RWGS-active palladium nanoparticles of up to 5 nm in size was observed. DFT calculations helped to rationalize the profoundly diverse time-on-stream behaviors of the two materials. They indicated that palladium accommodated onto the surface preferentially locates in depressions of the  $In_2O_3(111)$  termination ( $Pd_{pocket}$  in Fig. 3a), but remains very mobile and freely agglomerates. In stark contrast, palladium embedded into the oxide structure ( $Pd_{lattice}$  in Fig. 3a) serves as effective anchoring site for the noble-metal atoms accommodated onto the surface, hindering excessive sintering. Intrigued by the selectivity–nuclearity correlation observed experimentally, we analyzed a larger range of surface configurations with progressively more palladium atoms exposed on the surface. We found that models with 1–2 exposed palladium atoms per unit cell are selective towards methanol to a greater extent than bulk indium oxide, while, for models with 3 exposed Pd atoms, the intrinsic activity of palladium for the RWGS reaction is dominant and CO is the favored product overall (Fig. 3b). Nevertheless, as the methanol selectivity in the coprecipitated catalyst remained

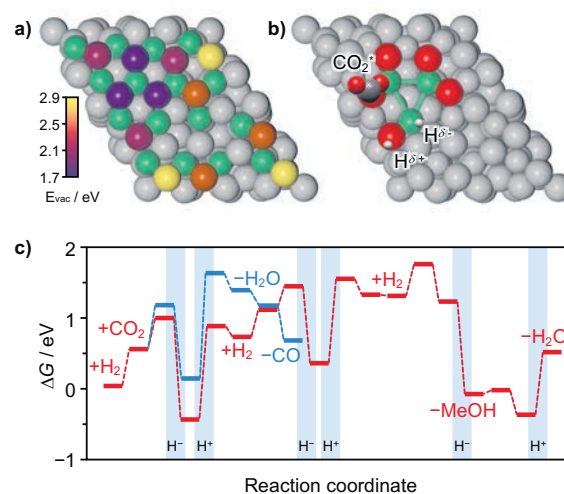


Fig. 2. a) The pristine  $In_2O_3(111)$  termination with surface oxygen atoms colored according to the energy required to abstract them leading to a vacancy ( $E_{vac}$ ), and b) adsorption geometry of  $CO_2$  and  $H_2$  on the  $In_3O_5$  ensemble arising when the energetically most favorable vacancy is formed. c) Gibbs energy profile for the hydrogenation of  $CO_2$  to MeOH (red) and CO (blue) through their most relevant paths, with steps involving proton or hydride transfers highlighted. Conditions:  $P = 5$  MPa,  $T = 573$  K.

Table 1. Apparent activation energies ( $E_{a,i}$ ) and reaction orders of reactants and products ( $n$ ) for  $In_2O_3$ -based catalysts.

Catalyst <sup>a</sup>	$E_{a,MeOH}$ [kJ mol <sup>-1</sup> ]	$E_{a,CO}$ [kJ mol <sup>-1</sup> ]	$n_{H_2}$ [–]	$n_{CO_2}$ [–]	$n_{H_2O}$ [–]	$n_{MeOH}$ [–]
$In_2O_3$	106 ± 6	118 ± 9	0.5–0.8	–0.1	–0.8	–0.2
$In_2O_3/m-ZrO_2$ -WI <sup>a</sup>	89 ± 4	112 ± 5	0.3	0	–0.5	–0.2
$In_2O_3/t-ZrO_2$ -WI <sup>a</sup>	103 ± 4	120 ± 6	0.5	–0.1	–0.8	–0.1
Pd- $In_2O_3$ -CP <sup>a</sup>	84 ± 5	119 ± 8	–0.1	0.2	–0.3	–0.5
Pd- $In_2O_3$ -DI <sup>a</sup>	83 ± 6	108 ± 7	–0.1	0.3	–0.2	–0.9

<sup>a</sup>WI: wet impregnation, CP: coprecipitation, DI: dry impregnation.

unaltered, the formation of the latter configuration was likely prohibited by the intrinsically low amount of palladium incorporated in the catalyst.

Evaluation of kinetic data was in support of the predicted structure–performance relationship. In the case of the CP catalyst, the apparent activation energy for CO<sub>2</sub> hydrogenation to methanol is *ca.* 20% lower than that previously estimated for pure In<sub>2</sub>O<sub>3</sub> (Table 1), whereas that of the RWGS reaction is equivalent. In contrast, the activation energy for the parasitic reaction is lower for the DI catalyst, due to the concomitant participation of the palladium nanoparticles in CO<sub>2</sub> conversion. Matching our expectations, the reaction order with respect to hydrogen was lowered to a value close to 0, implying that this catalyst could be operated in a hydrogen-lean feed. In view of above-discussed LCA data, this promises an easier transition towards industrialization. Moreover, a less inhibiting effect of water relieves the constraints imposed by its separation from a recycle stream and hints at a higher resistance against sintering induced by this compound. Overall, applying the optimal conditions identified in the kinetic analysis ( $H_2:CO_2 = 4$ ,  $P = 5$  MPa,  $T = 553$  K, and  $WHSV = 48,000$  cm<sup>3</sup><sub>STP</sub> h<sup>-1</sup> g<sub>cat</sub><sup>-1</sup>), a record methanol productivity of 0.96 g<sub>MeOH</sub> h<sup>-1</sup> g<sub>cat</sub><sup>-1</sup> was attained and sustained for 500 h on stream at a 60% lower residence time compared to pure In<sub>2</sub>O<sub>3</sub>. The latter condition implies a reduction of the reactor volume and the recycle stream by the same extent, bringing further advantages toward a large-scale application of the process.

### Role of the ZrO<sub>2</sub> Support

To rationalize the superiority of ZrO<sub>2</sub> as a support for In<sub>2</sub>O<sub>3</sub>, we set out to gain deeper fundamental understanding of electronic, geometric, and interfacial effects exerted by the carrier on the ac-

tive phase.<sup>[10]</sup> Fostering the contact between the two phases *via* a CP synthesis, generating In-Zr mixed oxides, did not yield better performing materials, which excludes a primary contribution of electronic effects. Interestingly, however, only 1 mol% of indium added in the catalyst preparation sufficed to stabilize zirconia in its metastable tetragonal phase. This effect, as well as the close structural matching of the cubic In<sub>2</sub>O<sub>3</sub> phase to both tetragonal (*t*) and monoclinic (*m*) ZrO<sub>2</sub>, prompted us to further investigate the impact of the carrier in materials prepared by wet impregnation, *i.e.* a deposition synthesis (Fig. 4). While X-ray diffraction did not evidence any reflection specific to In<sub>2</sub>O<sub>3</sub>, <sup>115</sup>In nuclear magnetic resonance spectroscopy, probing the short-range environment of indium, indicated that the oxide had a crystalline cubic structure over both supports. Putting forward that this is due to epitaxial alignment to the ZrO<sub>2</sub> carrier, detailed microscopy investigations were conducted, which revealed In atoms accommodated on top of columns of zirconium atoms as isolated species and/or forming two-dimensional subnanometric islands in In<sub>2</sub>O<sub>3</sub>/*m*-ZrO<sub>2</sub>. Temperature-programmed reduction with H<sub>2</sub> evidenced a considerably higher number of vacancies on In<sub>2</sub>O<sub>3</sub> carried on monoclinic zirconia, which could arise from the less perfect lattice matching between In<sub>2</sub>O<sub>3</sub> and this zirconia polymorph, causing tensile forces in the active phase. UV-vis spectroscopy corroborated this conclusion, evidencing a significantly lowered optical band gap for In<sub>2</sub>O<sub>3</sub> supported on this carrier. Based on observations made in semiconductor research, epitaxial strain indeed is linked a lower band gap and the formation of additional oxygen defects.<sup>[12]</sup> Catalytic testing revealed a far superior indium-specific activity for In<sub>2</sub>O<sub>3</sub>/*m*-ZrO<sub>2</sub>, whereas the catalyst based on *t*-ZrO<sub>2</sub> performed equivalently to the pure oxide benchmark, suggesting that the catalytic properties of In<sub>2</sub>O<sub>3</sub> are not substantially altered when the

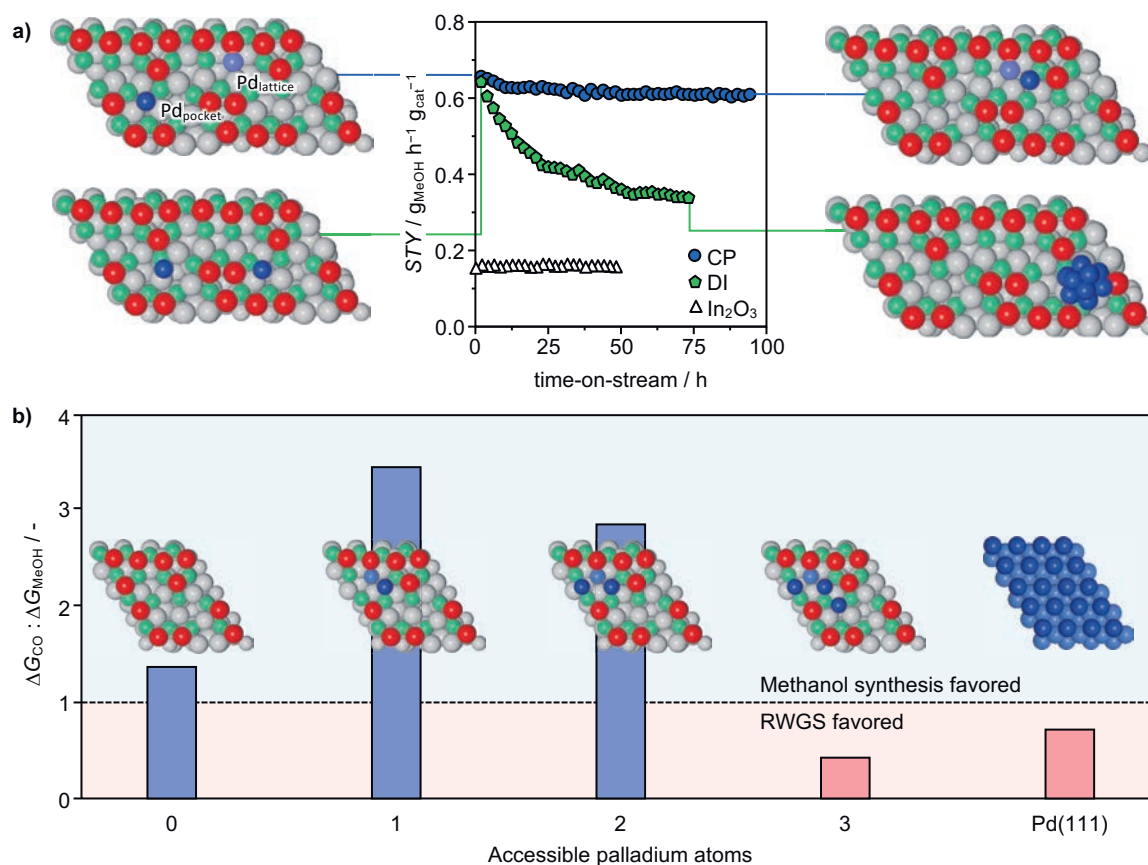


Fig. 3. a) Temporal evolution of the methanol space-time yield (STY) of coprecipitated (CP) and dry-impregnated (DI) Pd/In<sub>2</sub>O<sub>3</sub> catalysts, with pure In<sub>2</sub>O<sub>3</sub> serving as a reference. The structures to the left and right are representative for the surface arrangement of atoms of the solids before and after the reaction. b) Ratio of the computed activation energies for methanol synthesis ( $\Delta G_{MeOH}$ ) and reverse water-gas shift ( $\Delta G_{CO}$ ) over catalyst surfaces with increasing nuclearity of exposed palladium. Values greater or smaller than 1 indicate a preferential selectivity towards methanol or CO, respectively. Conditions:  $T = 553$  K,  $P = 5$  MPa,  $H_2:CO_2 = 4$ , and  $WHSV = 24,000$  cm<sup>3</sup><sub>STP</sub> h<sup>-1</sup> g<sub>cat</sub><sup>-1</sup>.

latter support is used. In line with this, lower activation barriers for methanol synthesis and the RWGS reaction and a reduced dependency on the hydrogen concentration in the feed were determined for  $\text{In}_2\text{O}_3$  carried on the monoclinic support, while kinetic parameters for  $\text{In}_2\text{O}_3/t\text{-ZrO}_2$  are equivalent to those of pure  $\text{In}_2\text{O}_3$  (Table 1). The experiments also revealed a less detrimental effect of water on the reaction as well as on the catalyst structure in  $\text{In}_2\text{O}_3/m\text{-ZrO}_2$ , explaining its high stability. The variation in activation energy and reaction orders speaks for a diverse nature of the active ensembles, *i.e.* a second oxygen atom could be abstracted in their proximity forming a more effective  $\text{In}_3\text{O}_4$  ensemble, or  $\text{ZrO}_2$  may take direct part in the mechanism aiding the activation of  $\text{CO}_2$ . A significantly higher  $\text{CO}_2$  storage capacity for the monoclinic carrier, as well as the exclusive generation of formate species on  $\text{In}_2\text{O}_3/m\text{-ZrO}_2$  corroborate a contribution of such interfacial active site. Further studies, making use of model catalysts with precise geometries of active and supporting phases shall be instrumental to unravel the contribution of the two synergetic centers.

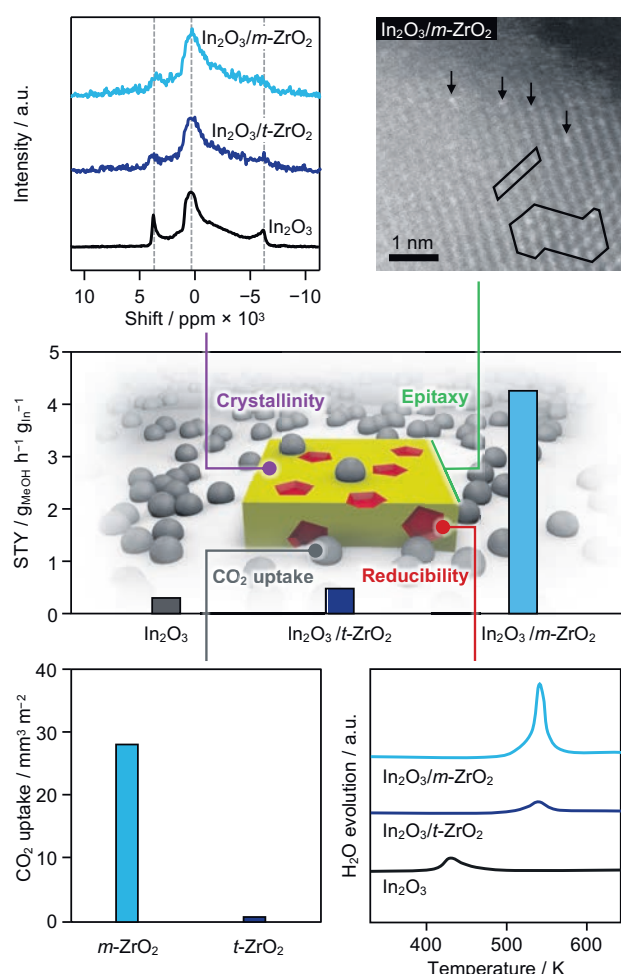


Fig. 4. Center: Indium-specific methanol space-time yield for  $\text{In}_2\text{O}_3$  supported on tetragonal (*t*) and monoclinic (*m*) zirconia, with the pure oxide serving as a reference. The inset shows a schematic representation of the catalytic system with key techniques applied to elucidate specific structural and chemical properties. Top to bottom, left to right:  $^{115}\text{In}$  solid state nuclear magnetic resonance spectroscopy, aberration-corrected high-resolution transmission electron microscopy, volumetric chemisorption of  $\text{CO}_2$ , and temperature-programmed reduction by  $\text{H}_2$ . Individual indium atoms and islands are marked in the micrograph. Conditions:  $T = 553\text{ K}$ ,  $P = 5\text{ MPa}$ ,  $\text{H}_2:\text{CO}_2 = 4$ , and  $\text{WHSV} = 24,000\text{ cm}^3_{\text{STP}}\text{ h}^{-1}\text{ g}_{\text{cat}}^{-1}$ .

## Conclusions and Outlook

In this contribution, we have highlighted how a recent frontier system engineering analysis highlights that a  $\text{CO}_2$ -based methanol synthesis process would contribute to a more sustainable planet and would become economically more attractive if the  $\text{CO}_2$  and  $\text{H}_2$  feedstocks were cheaper and efficiently converted by a suitable catalytic material. In this regard, we have reviewed the steps made in the development and understanding of  $\text{In}_2\text{O}_3$ -based catalysts that hold promise for industrialization. A combined kinetic and density functional theory analysis of the pure indium oxide elucidated the mechanistic origin of the high methanol selectivity imparted by oxygen vacancies acting as active sites in the material and pointed to hydrogen activation and resilience towards water-induced sintering as key optimization parameters. Addressing the former, we showed that indium oxide can be successfully promoted by palladium if the noble metal is added through controlled coprecipitation, which leads to low-nuclearity palladium clusters anchored into the  $\text{In}_2\text{O}_3$  lattice. In contrast to the palladium nanoparticles obtained by classical impregnation, these species do not excessively agglomerate and are not active in the reverse water-gas shift reaction, thus exclusively supporting methanol synthesis. Furthermore, we have attributed the superiority of monoclinic  $\text{ZrO}_2$  as a support for  $\text{In}_2\text{O}_3$  to a delicate mismatch between the lattices of these two oxides, leading to epitaxial strain exerted on  $\text{In}_2\text{O}_3$ , which generates additional and potentially more active ensembles. The ability of  $\text{ZrO}_2$  to activate  $\text{CO}_2$  and its cooperation with  $\text{In}_2\text{O}_3$  at interfacial sites is put forward as a second origin for the activity boost. The epitaxial alignment of  $\text{In}_2\text{O}_3$  to the  $\text{ZrO}_2$  lattice also explains the outstanding stability of this catalyst. Overall, detailed characterization coupled to thorough experimental investigation of the reaction kinetics and density function theory simulations enabled us to unravel the nature of the active sites in palladium-promoted and zirconia-supported  $\text{In}_2\text{O}_3$  catalysts at an atomic scale. This work paves the way to develop and further improve a system offering superior performance and stability in a perspective large-scale application, a dedicated effort currently underway in our group.

## Author contributions

The manuscript was written through contributions of all authors. All authors have given approval to the final version of the manuscript.

## ORCID

Cecilia Mondelli: 0000-0003-3917-6794  
Javier Pérez-Ramírez: 0000-0002-5805-7355

## Notes

The authors declare no competing financial interest.

## Acknowledgements

The authors express special gratitude to Dr. Joseph A. Stewart and Dr. Daniel Curulla Ferré from Total Research and Technology Feluy (TRTF) for the long-standing fruitful collaboration and TRTF for financial support. Prof. Dr. Gonzalo Guillén Gosálbez, Andrés González-Garay, Dr. Sharon Mitchell, and Dr. Frank Krumeich from ETH Zurich, Prof. Dr. Núria López, Dr. Marçal Capdevila-Cortada, and Dr. Rodrigo García-Muelas from the Institute of Chemical Research of Catalonia, Dr. Olga Safonova from the Paul Scherrer Institute, and Dr. Roland Hauert from Empa are also greatly acknowledged for their contributions to the research presented in this article and the insightful discussions.

Received: February 27, 2020

- [1] N. Mac Dowell, P. S. Fennell, N. Shah, G. C. Maitland, *Nat. Clim. Change* **2017**, 7, 243, doi: 10.1038/nclimate3231.
- [2] M. D. Porosoff, B. Yan, J. G. Chen, *Energ. Environ. Sci.* **2016**, 9, 62, doi: 10.1039/c5ee02657a.
- [3] A. Behr, *Angew. Chem., Int. Ed.* **2014**, 53, 12674, doi: 10.1002/anie.201409583.

- [4] A. González-Garay, M. S. Frei, A. Al-Qahtani, C. Mondelli, G. Guillén-Gosálbez, J. Pérez-Ramírez, *Energ. Environ. Sci.* **2019**, *12*, 3425, doi: 10.1039/C9EE01673B.
- [5] K. Sun, Z. Fan, J. Ye, J. Yan, Q. Ge, Y. Li, W. He, W. Yang, C.-j. Liu, *J. CO<sub>2</sub> Util.* **2015**, *12*, 1, doi: 10.1016/j.jcou.2015.09.002.
- [6] J. Ye, C. Liu, Q. Ge, *J. Phys. Chem. C* **2012**, *116*, 7817, doi: 10.1021/jp3004773.
- [7] O. Martín, A. J. Martín, C. Mondelli, S. Mitchell, T. F. Segawa, R. Hauert, C. Drouilly, D. Curulla Ferré, J. Pérez-Ramírez, *Angew. Chem., Int. Ed.* **2016**, *55*, 6261, doi: 10.1002/anie.201600943.
- [8] M. S. Frei, M. Capdevila-Cortada, R. García-Muelas, C. Mondelli, N. López, J. A. Stewart, D. Curulla Ferré, J. Pérez-Ramírez, *J. Catal.* **2018**, *361*, 313, doi: 10.1016/j.jcat.2018.03.014.
- [9] M. S. Frei, C. Mondelli, R. García-Muelas, K. S. Kley, B. Puértolas, N. López, O. V. Safonova, J. A. Stewart, D. Curulla Ferré, J. Pérez-Ramírez, *Nat. Commun.* **2019**, *10*, 3377, doi: 10.1038/s41467-019-11349-9.
- [10] M. S. Frei, C. Mondelli, A. Cesarini, F. Krumeich, R. Hauert, J. A. Stewart, D. Curulla Ferré, J. Pérez-Ramírez, *ACS Catal.* **2020**, *10*, 1133, doi: 10.1021/acscatal.9b03305.
- [11] D. Albani, M. Capdevila-Cortada, G. Vile, S. Mitchell, O. Martín, N. López, J. Pérez-Ramírez, *Angew. Chem., Int. Ed.* **2017**, *56*, 10755, doi: 10.1002/anie.201704999.
- [12] A. Walsh, C. R. A. Catlow, K. H. L. Zhang, R. G. Egdell, *Phys. Rev. B* **2011**, *83*, 161202, doi: 10.1103/PhysRevB.83.161202.

#### License and Terms



This is an Open Access article under the terms of the Creative Commons Attribution License CC BY\_NC 4.0. The material may not be used for commercial purposes.

The license is subject to the CHIMIA terms and conditions: (<http://chimia.ch/component/sppagebuilder/?view=page&id=12>).

The definitive version of this article is the electronic one that can be found at doi:10.2533/chimia.2020.257